Hindawi
Journal of Food Quality
Volume 2023, Article ID 8230958, 17 pages
https://doi.org/10.1155/2023/8230958

Research Article

Systematic Characterization of the Chemical Components of *Canna edulis* Ker-Gawl Based on UHPLC Q-Exactive Orbitrap MS Technology

Liqiao Lv,[1] Chi Zhang,[1] Jiahui Wu,[1] Dachuan Zhang,[1] Fangyuan Zhao,[1] Lv Bu Aga,[1] Nan Wang,[1] Junling Li,[1] Leimengyuan Tang,[1] Baosheng Zhao,[2] Chunguo Wang,[2] and Xueyong Wang [1,2]

[1]*School of Chinese Materia Medica, Beijing University of Chinese Medicine, Northeast Corner of Intersection of Sunshine South Street and Baiyang East Road, Fang-Shan District, Beijing 102488, China*
[2]*Beijing Institute of Chinese Medicine, Beijing University of Chinese Medicine, Beijing 102488, China*

Correspondence should be addressed to Xueyong Wang; wxyph.d@163.com

Received 18 August 2022; Revised 29 January 2023; Accepted 5 April 2023; Published 2 May 2023

Academic Editor: Ali Akbar

Canna edulis Ker-Gawl is a versatile crop that integrates food, energy, and feed in China. The rhizome is a traditional Chinese medicine with a long history. However, there are few studies on chemical components. Crude plant extracts are a complex mixture of several biologically active secondary metabolites. Therefore, rapid and accurate identification and quantification are critical in phytochemical analysis. An efficient approach based on ultrahigh-performance liquid chromatography coupled with Q-Exactive Orbitrap tandem mass spectrometry (UHPLC Q-Exactive Orbitrap MS) was used to analyze the chemical components systematically. We used retention time, accurate molecular weight, parent peaks, fragment peaks, fragmentation characteristics, comparative analysis with the literature, reference standards, and standard databases, including ChemSpider, mzVault, MassBank, and mzCloud. A total of 54 chemical constituents were identified from the methanol extract of the rhizome, including 36 organic acids (with six phenolic acids), three phenols, one sugar (and its derivatives), one coumarin, one triterpenoid, ten N-containing organic compounds (including seven amino acids), and two other compounds. Moreover, three compounds were quantitatively analyzed and a methodological study of the three components was carried out. The established method provided satisfactory precision and accuracy, acceptable recovery, good linearity, and a reasonable detection limit. The UHPLC Q-Exactive Orbitrap MS method was used for the first time to accurately, quickly, and systematically characterize the compounds of the rhizome, revealing the pharmacodynamic substances and providing a theoretical basis for its quality control, in-depth research, and development.

1. Introduction

Canna edulis Ker-Gawl is a perennial herb from the genus *Caanna* (Cannaceae). *Canna edulis* is rich in germplasm resources, which can be found in Guizhou province, Yunnan province, Guangxi province, and other places [1]. The rhizome of *Canna edulis* Ker-Gawl is shown in Figure 1. It is a traditional herb used as medicine and food in China with considerable economic, social, ecological, and medicinal benefits. The herb contains rich trace elements, amino acids, vitamins, and other nutrients [2–4]. The dry rhizome contains 70–80 g/100 g of starch [5, 6] that is commonly used for functional food and dietary fiber [7–11] or fermentation of industrial alcohols [12–14].

Canna edulis Ker-Gawl was listed as a classical medicinal plant in "Miao medicine" and "Dai medicine," a branch of traditional Chinese medicine (TCM). It is also called "jiao-yu," "jiang-yu" (Guangdong Province), "Jiang-ya" (Guangdong, Guizhou Province), "Ba-jiao-ya," "Xiang-zhu," "Man-dong" (Dai Medicine), "Hong-jiang-qi" (Miao Medicine), and "Han-ou" in ethnopharmacology. TCM has accumulated information on the use of the herb in ancient manuscripts

Figure 1: The rhizome of *Canna edulis* Ker-Gawl.

and recently published books, including "Zi Yuan Zhi," "Xiang Lan Kao," "Dian Yao Lu," "Dai Yao Lu," "Gui Yao Bian," and "Zhong Hua Ben Cao." According to ancient Chinese herbal literature, *Canna edulis* Ker is sweet and light and has a cold nature. The rhizome clears heat and dampness, protects the liver and gallbladder, cools the blood and detoxifies, and invigorates the spleen and stomach (derived from: http://www.plant.csdb.cn/herb). In China, the herb has been used as a local medicine to treat dysentery, diarrhea, acute icteric hepatitis, metrorrhagia, leukorrhea, irregular menstruation, hemoptysis, and sore swollen poison syndrome.

Modern pharmacological studies have found that *Canna edulis* Ker -Gawl protects the liver and gallbladder, treats acute jaundice hepatitis, has a gastroprotective effect [15], lowers blood pressure, lowers blood glucose, lowers blood lipids, prevents colon cancer [16], and cardiovascular disease [17, 18] and has antioxidant activities [19, 20]. Previous studies from our group [21–25] found that the resistant starch from the rhizome of *Canna edulis* Ker (Ce-RS3) after 11 weeks of Ce-RS3 intervention showed antidiabetic effects similar to metformin, significantly reduced blood glucose, reduced insulin resistance, increased glucose tolerance, and reduced pathological damage. In addition, Ce-RS3 significantly reduced body weight and dyslipidemia in obese mice.

Studies on *Canna edulis* Ker-Gawl have focused on cultivation, starch extraction, transformation, and utilization [26–28], and there are few studies on its chemical composition. Only about thirty monomers have been obtained by systematic phytochemical enrichment and separation [29]. For example, through the analysis of the chemical components of the ethyl acetate-soluble residue of the methanolic extract derived from dry rhizomes of *Canna edulis*, Young Sook Yun et al. [30] isolated two phenylpropanoid sucrose esters together with a known phenylpropanoid sucrose ester and four known phenylpropanoids, i.e., caffeic acid, rosmarinic acid, caffeoyl-4′-hydroxyphenyllactic acid, and salvianolic acid B. Through the analysis of the residue of *Canna edulis*, Zhang et al. [31] isolated 11 compounds from water-soluble extract, i.e., rosmarinic acid, salvianolic acid B, ferulic acid, caffeic acid, 1-caffeoylquinic acid, 3-caffeoylquinic acid, 4-caffeoylquinic acid, 5-caffeoylquinic acid, salicylic acid, and gallic acid. Moreover, by analyzing and summarizing a large number of documents, Zhang et al. [32] reviewed the chemical constituents of *Canna edulis* and found that the main secondary metabolites of are phenolic compounds.

With the development of the pharmaceutical health and food industry, increasing attention has been paid to the study of *Canna edulis* Ker -Gawl. UHPLC Q-Exactive Orbitrap MS has excellent resolution, sensitivity, and performance and enables rapid compound identification, structure confirmation, and quantitative target analysis [33, 34]. Therefore, for the first time we used UHPLC Q-Exactive Orbitrap MS analysis technology to perform a comprehensive and systematic chemical composition analysis to provide a basis for further research and development of medicinal substances and quality control.

2. Materials and Methods

2.1. Instruments and Software. UHPLC Q-Exactive Orbitrap MS system: Vanquish Flex UHPLC series Q-Exactive high-resolution mass spectrometer (Themo Fisher Scientific, USA), Ultrasonic apparatus (Shenzhen Guanyijia Technology Co., LTD.), Electronic Balance (Cedis Scientific Instruments (Beijing) Co., Ltd.), Centrifuge (Hunan Xiangyi Laboratory Instrument Development Co., LTD.), Xcalibur 4.4 Workstation (Themo Fisher Scientific, USA), Compound Discoverer3.1 Compound Analysis and Identification Software (Thermo Fisher Scientific, USA), CORTECS UPLC C_{18} column (2.1 × 100 mm, 1.6 μm) was purchased from Waters.

2.2. Reagents and Materials. Methanol, Acetonitrile, Formic acid were both in mass grade, which were purchased from Thermo Fisher & Fisher Technology Co., Ltd. (China).

Distilled Water was obtained from Guangzhou Watsons Food & Beverage Co., Ltd. (China).

Caanna edulis Ker comes from Xingyi medicinal materials planting base, Guizhou Province, acquired in November 2021 and identified as the rhizome of *Canna edulis* Ker by professor Liu Chunsheng of Beijing University of Chinese Medicine.

Caffeic acid (purity ≥ 98%), ferulic acid (purity ≥ 98%), quinic acid (purity ≥ 98%), citric acid (purity ≥ 98%), and palmitic acid (purity ≥ 98%) were obtained from Shanghai Yuanye Biotechnology Co., Ltd. (China).

2.3. Preparation of Sample and Reference Solutions. 20 g of *Canna edulis* Ker powder was accurately weighed by electronic analytical balance. After 10 mL of methanol was added, an extract was obtained by sonication for 2 h at 25°C. The supernatants were centrifuged at 12 000 r·min^{-1} for 10 min. Then, using a pipette to remove and filter through a 0.22 μm nylon millipore filter and added to the liquid vial for further analysis.

The reference solutions including caffeic acid, ferulic acid, quinic acid, citric acid, and palmitic acid were dissolved in methanol with appropriate amounts, respectively, as a single control reserve liquid. All the reference solutions were stored at 4°C before analysis.

2.4. Chromatographic Conditions. The UHPLC separation was performed on Vanquish Flex UHPLC System (Thermo Fisher Scientific, San Jose, CA, USA) with a Waters CORTECS UPLC C_{18} column (2.1 × 100 mm, 1.6 μm) maintained at 35°C. Mobile phases were acetonitrile (A) and 0.1% formic acid aqueous solution (B), with the following gradient elution procedure: 0 min, 10% A; 0 ⟶ 4 min, 10% ⟶ 23% A; 4 ⟶ 15 min, 23% ⟶ 41% A; 15 ⟶ 31 min, 41% ⟶ 90% A; 31 ⟶ 33 min, 90% A; 33-33.1 min, 90% ⟶ 10% A; 33.1 ⟶ 34 min, and 10% A. The flow rate of elution solvent was 0.3 mL·min^{-1} and injection volume of samples was 5 μL.

2.5. Mass Spectrometry Conditions. MS detection was carried out under the positive and negative ion mode with heated electrospray ionization (HESI) source. The scan mode was full scan/dd MS^2. The mass range and the mass resolution were set at 100–1 200 Da and 70 000 FWHM. The operating parameters for positive ionization mode were: spray voltage 3 800 V and capillary temperature 350°C. The flow rate of sheath gas and auxiliary gas were set to 35, 15 (arbitrary units), respectively. As for the negative ionization mode, the operating parameters were as following: spray voltage 3 000 V and capillary temperature 320°C. The flow rate of sheath gas and auxiliary gas were set to 35 and 10 (arbitrary units), respectively.

2.6. Methodological Validation of the Quantitative Analysis. The quantitative analysis established in this study was validated regarding linearity, limit of detection (LOD), and quantification (LOQ), precision and recovery.

2.6.1. Preparation of the Standard Solutions, Linearity, and Sensitivity. We prepared *D*- (-)-quinic acid, caffeic acid, and ferulic acid stock solutions at 20 mM, respectively. A series calibration standard solutions were prepared by diluted and mixed stock solutions. In order to plot calibration curves, seven standard working solutions at different concentrations were achieved by serially mixing and diluting the stock solutions. The molar concentrations of each component to be measured were quinic acid 0.781 μM, 1.563 μM, 3.125 μM, 6.250 μM, 12.500 μM, 25.000 μM, and 50.000 μM; caffeic acid 7.813 μM, 15.625 μM, 31.250 μM, 62.500 μM, 125.000 μM, 250.000 μM, and 500.000 μM; ferulic acid 0.260 μM, 0.521 μM, 1.042 μM, 2.084 μM, 4.168 μM, 8.335 μM, and 16.667 μM. The calibration curves were constructed by plotting peak area (y) against concentration (x, μM). The LODs and LOQs were determined based on the signal-to-noise (S/N) of 3 and 10, respectively.

2.6.2. Precision. The intraday precision for each compound was determined by analyzing one standard solution samples ($n = 6$) on the same day (intraday).

2.6.3. Accuracy and Recovery. The standard compound mixtures in three different concentrations (low, middle and high) at known and particular concentrations were added into corresponding untreated samples. The samples were treated and analyzed as described above to determine recoveries of the three components. Three parallel samples were prepared. The RSD% of the areas and contents were calculated. The data were input into GraphPad Prism (version 9.0) for the quantification analysis.

2.7. Data Analysis. Data acquisition and processing were based on the elemental compositions of the precursors. Raw mass spectrum data collected were imported into Compound Discoverer 3.1 (Thermo Fisher Scientific, USA) for data processing. We recorded peak extraction, retention time correction within and between groups, additive ion merging, missing value filling, background peak labeling, and metabolite identification. To identify compounds, we compared the information to databases, including ChemSpider, mzVault, MassBank database (http://www.massbank.jp/Index), and mzCloud (https://www.mzcloud.org/). Then, the exact mass coupled with MS/MS spectrum was matched with the library databases. Finally, the fragmentation patterns of components were illustrated using ChemDraw (version 18.0). For the quantification analyze, the data were input into Graphpad Prism (version 9.0).

3. Results

3.1. Base Peak Ion Chromatogram. The base peak chromatogram of *Caanna edulis* Ker -Gawl and references are shown in Figure 2.

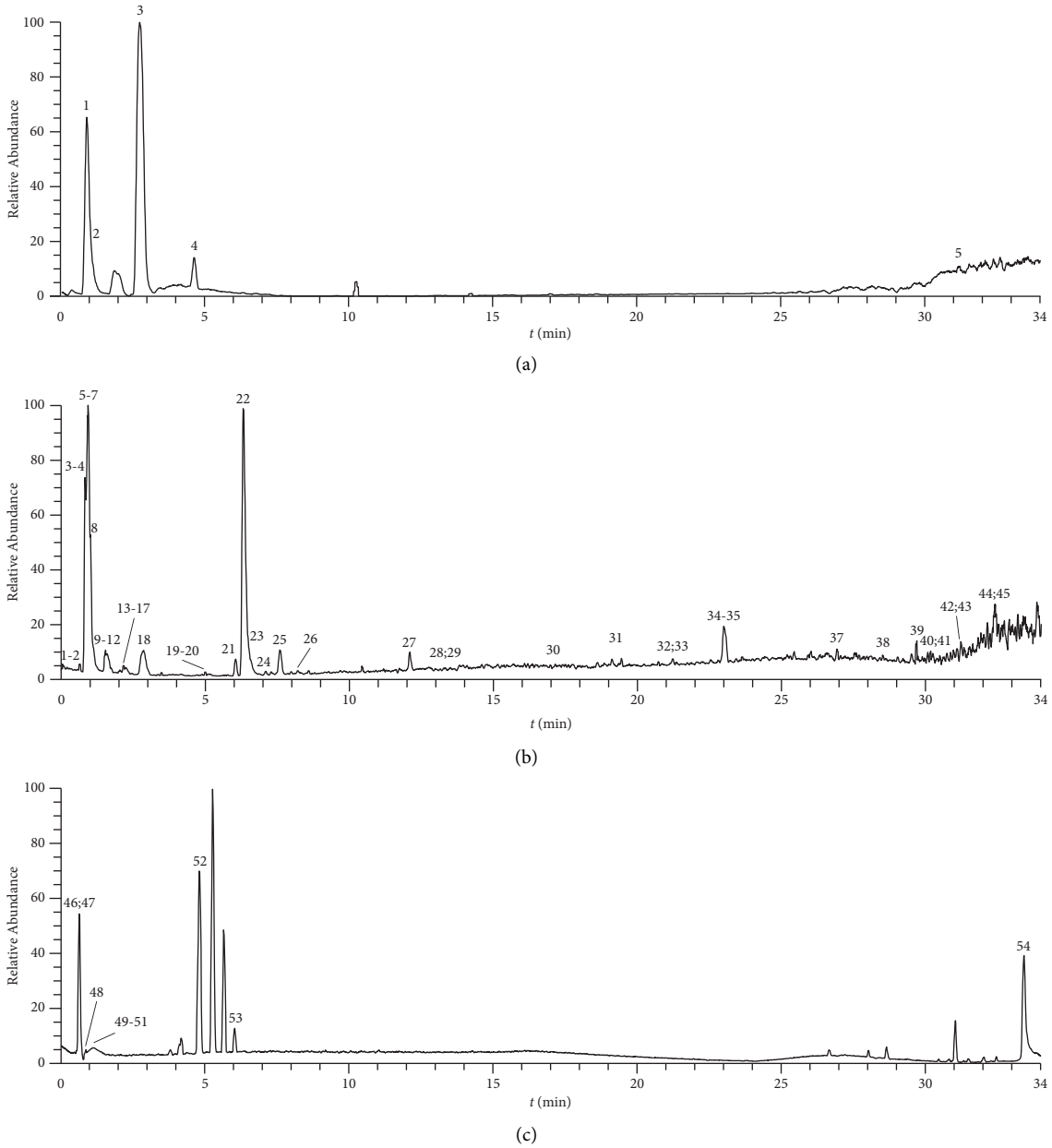

Figure 2: Base peak chromatography of references (a) and *Canna edulis* Ker in the negative (b) and positive (c) ion mode.

3.2. Identification Results of Chemical Composition. UHPLC Q-Exactive Orbitrap MS was used for components profiling of the methanol extract of the rhizome of *Canna edulis* Ker-Gawl. Fifty-four chemical constituents were identified from the methanol extract of the rhizome, with 36 organic acids (including six phenolic acids), three phenols, one sugar (and its derivatives), one coumarin, one triterpenoid, ten N-containing organic compounds (including seven amino acids), and two other compounds. The retention time, molecular ion peak, molecular weight, molecular formula, and proposed compounds are presented in Table 1. Our results from UPLC-LTQ-Orbitrap-MS showed that accurate mass error values were below 5 ppm.

3.3. Identification Process. The identification process of the compounds was as follows.

3.3.1. Organic Acids. We identified 36 organic acid components, including six phenolic acids. Organic acids contain -COOH functional groups that are likely to remove small molecule groups such as H_2O, CO_2, and $-CH_3$. We took peaks 3, 5, 7, 8, 11, 13, 14, 15, 18, and 20 as examples to explain its lysis rules.

Peak 20, t_R 4.650, $C_{10}H_{10}O_4$, was deprotonated in the negative ion mode to produce ion m/z 193.050 51 $[M\text{-}H]^-$, then lost a CH_3·group and obtained ion 178.027 33 $[M\text{-}H\text{-}CH_3\cdot]^-$, or lost a CO_2 group and obtained ion 149.024 55 $[M\text{-}H\text{-}CO_2]^-$. If both CH_3· and CO_2 were lost, the fragment of

Table 1: Identification of chemical components in *Canna edulis* Ker based on UHPLC Q-Exactive Orbitrap MS.

No.	Compound	t_R(min)	Formula	Measured value (*m/z*)	Theoretical value (*m/z*)	Error (ppm)	Fragment ions (*m/z*)	Mode	Compound type	Structure
1	*α, α*-Trehalose	0.834	$C_{12}H_{22}O_{11}$	341.109 10	341.107 84	0.490	341.108 98; 179.056 08; 161.045 50; 143.034 90; 119.034 90; 113.024 42; 101.024 35; 89.024 41; 71.013 82; 59.013 84;	Neg	Sugars and their derivatives	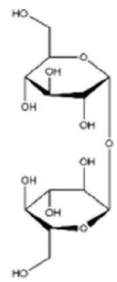
2	*D*- (-)-Glutamine	0.840	$C_5H_{10}N_2O_3$	145.061 83	145.060 77	−0.250	145.061 77; 127.051 22; 128.035 29; 125.035 48; 109.040 73; 102.055 89; 101.071 80; 84.045 46;	Neg	Amino acids	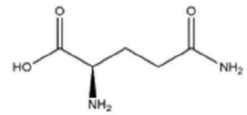
3*	*D*- (-)-quinic acid	0.951	$C_7H_{12}O_6$	191.056 12	191.055 01	0.050	191.056 12; 173.045 41; 127.039 98; 111.008 74; 87.008 74; 85.029 48	Neg	Organic acids	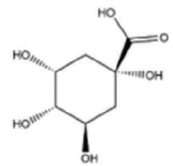
4	Asparagine	0.978	$C_4H_7NO_4$	131.045 94	131.046 22	−0.140	131.045 94; 114.019 65; 113.035 70; 111.020 13; 87.056 59; 72.009 07; 70.029 80	Neg	Amino acids	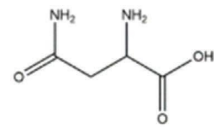
5*	Citric acid	1.000	$C_6H_8O_7$	191.019 74	191.019 74	0.180	173.046 17; 146.938 60; 129.019 18; 111.008 75; 102.948 79; 87.008 76; 85.029 50	Neg	Organic acids	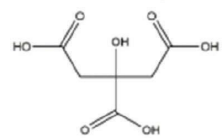
6	4-Oxoproline	1.117	$C_5H_7NO_3$	128.035 28	128.034 22	−0.180	88.040 49; 85.029 64; 82.029 90; 69.435 51; 57.034 45;	Neg	Amino acids	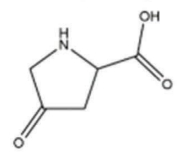
7	Succinic acid	1.126	$C_4H_6O_4$	117.019 33	117.018 24	−0.190	117.019 33; 99.008 74; 73.029 46	Neg	Organic acids	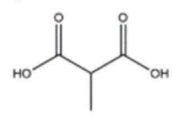

Table 1: Continued.

No.	Compound	t_R(min)	Formula	Measured value (*m/z*)	Theoretical value (*m/z*)	Error (ppm)	Fragment ions (*m/z*)	Mode	Compound type	Structure
8	Gallic acid	1.191	$C_7H_6O_5$	169.014 14	169.013 15	−0.330	169.014 14; 126.02801; 125.024 35; 124.040 34; 78.959 02	Neg	Organic acids/ phenolic acids	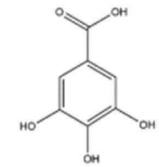
9	Pantothenic acid	1.318	$C_9H_{17}NO_5$	218.103 42	218.103 47	0.130	218.103 47; 146.082 24; 88.040 41; 71.013 82	Neg	Organic acids	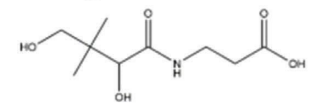
10	6-Methoxysalicylic acid	1.398	$C_8H_8O_4$	167.034 97	167.034 91	−0.050	167.034 91; 123.045 15	Neg	Organic acids/ phenolic acids	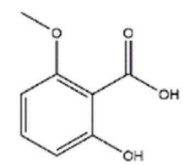
11	Catechol	1.595	$C_6H_6O_2$	109.029 49	109.028 41	−0.350	109.029 49; 108.021 55; 91.01882; 81.03461	Neg	Phenols	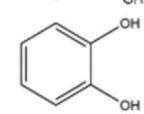
12	*DL*-4-hydroxyphenyllactic acid	1.745	$C_9H_{10}O_4$	181.050 67	181.049 54	−0.100	181.050 67; 163.040 07; 135.045 12; 119.050 11; 72.993 10	Neg	Organic acids/ phenolic acids	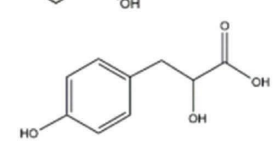
13	Malic acid	2.007	$C_4H_6O_5$	133.040 62	133.013 15	−0.530	133.040 62; 115.003 72; 89.024 44; 87.008 93; 72.993 24; 71.01396	Neg	Organic acids	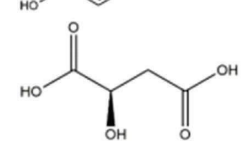
14	Malic acid	2.167	$C_4H_6O_5$	133.014 22	133.013 15	−0.530	133.014 22; 115.003 65; 89.024 48; 87.008 74; 72.993 16; 71.013 90	Neg	Organic acids	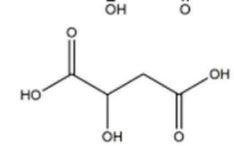
15	Gentisic acid	2.228	$C_7H_6O_4$	152.904 69	153.018 24	−0.090	153.019 32; 123.045 17; 109.029 45; 108.021 45	Neg	Organic acids/ phenolic acids	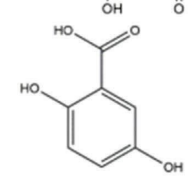
16	(*2R*)-2,3-dihydroxypropanoic acid	2.249	$C_3H_6O_4$	105.019 29	105.018 24	−0.490	105.019 29; 72.993 14; 59.013 87; 75.008 77	Neg	Organic acids	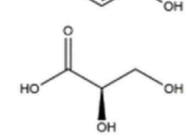

Table 1: Continued.

No.	Compound	t_R(min)	Formula	Measured value (*m/z*)	Theoretical value (*m/z*)	Error (ppm)	Fragment ions (*m/z*)	Mode	Compound type	Structure
17	*cis, cis*-Muconic acid	2.250	$C_6H_6O_4$	141.019 36	141.018 24	−0.100	141.019 36; 97.029 50; 95.013 83; 85.029 51; 69.034 58;	Neg	Organic acids	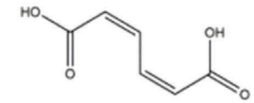
18*	Caffeic acid	2.859	$C_9H_8O_4$	179.034 96	179.034 98	−0.220	179.034 96; 135.045 18; 107.050 29; 89.024 47	Neg	Organic acids/ phenolic acids	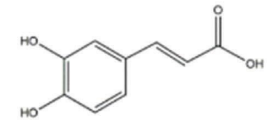
19	Suberic acid	4.345	$C_8H_{14}O_4$	173.081 85	173.080 84	−0.480	173.081 85; 155.035 19; 143.03535; 137.024 32; 129.092 24; 111.081 57; 93.034 56; 85.02959; 83.050 32; 73.029 48	Neg	Organic acids	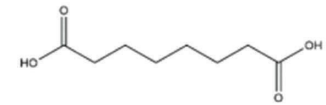
20*	Ferulic acid	4.650	$C_{10}H_{10}O_4$	193.050 51	193.049 54	−0.410	178.027 33; 161.024 49; 149.024 55; 137.024 52; 134.037 16; 121.029 27;	Neg	Organic acids/ phenolic acids	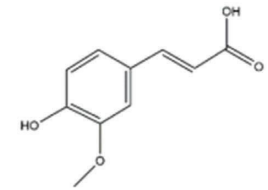
21	4-Oxo-4,5,6,7-tetrahydrobenzo[b] furan-3-carboxylic acid	5.696	$C_9H_8O_4$	179.034 67	179.033 89	−0.220	179.034 67; 135.045 29; 107.050 16; 89.024 48	Neg	Organic acids	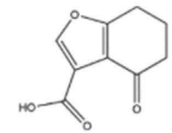
22	Azelaic acid	6.058	$C_9H_{16}O_4$	187.097 69	187.096 49	−0.170	187.097 69; 169.086 91; 143.107 54; 125.097 16; 97.065 89	Neg	Organic acids	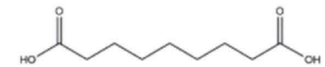
23	2-Methylbenzoic acid	6.329	$C_8H_8O_2$	135.045 20	135.044 06	−1.590	135.045 20	Neg	Organic acids	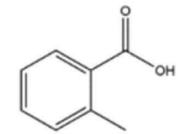
24	*δ*-Gluconic acid *δ*-lactone	7.107	$C_6H_{10}O_6$	177.019 27	177.039 36	−0.660	177.019 27; 158.925 38; 129.019 33; 99.008 79; 89.024 48; 71.013 82; 59.013 84	Neg	Organic acids	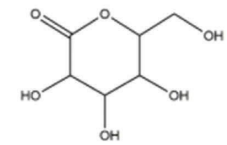
25	Pyrogallol	7.487	$C_6H_6O_3$	125.024 48	125.023 32	−0.150	125.02448; 107.013 95; 81.034 58; 97.029 53; 69.034 61	Neg	Phenols	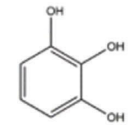

Table 1: Continued.

No.	Compound	t_R(min)	Formula	Measured value (*m/z*)	Theoretical value (*m/z*)	Error (ppm)	Fragment ions (*m/z*)	Mode	Compound type	Structure
26	3-tert-Butyladipic acid	7.986	$C_{10}H_{18}O_4$	201.113 25	201.112 14	0.320	201.113 25; 183.102 54; 157.051 21; 139.112 76	Neg	Organic acids	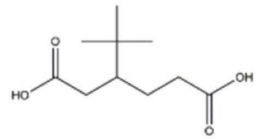
27	(*15Z*)-9,12,13-Trihydroxy-15-octadecenoic acid	12.097	$C_{18}H_{34}O_5$	329.233 64	329.232 25	0.800	329.233 64; 229.144 58; 211.134 11; 171.102 55; 139.113 13; 127.112 72; 99.081 63	Neg	Organic acids	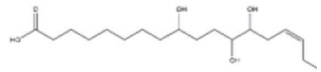
28	Tetradecanedioic acid	13.063	$C_{14}H_{26}O_4$	257.176 09	257.174 74	0.750	257.176 09; 239.165 28; 195.175 14; 167.14349; 83.050 31	Neg	Organic acids	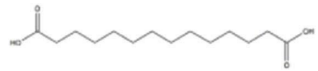
29	3-Hydroxydecanoic acid	13.412	$C_{10}H_{20}O_3$	187.097 67	187.132 87	0.020	187.09767; 59.013 87	Neg	Organic acids	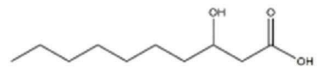
30	Corchorifatty acid F	17.458	$C_{18}H_{32}O_5$	327.217 90	327.216 60	0.600	327.217 90; 309.207 18; 291.196 41; 239.129 23; 229.144 67; 221.118 52; 213.11336; 211.134 25; 201.113 28; 183.139 31; 171.102 81; 113.09724; 97.065 84	Neg	Organic acids	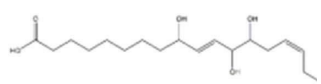
31	(±)12(13)-DiHOME	19.326	$C_{18}H_{34}O_4$	313.238 86	313.237 34	0.970	313.238 86; 295.227 97; 277.217 59; 195.139 13; 183.139 02; 129.092 12; 99.081 47	Neg	Organic acids	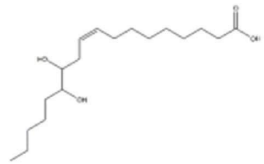
32	(±)9-HpODE	21.223	$C_{18}H_{32}O_4$	311.223 18	311.221 69	0.960	311.223 18; 293.212 43	Neg	Organic acids	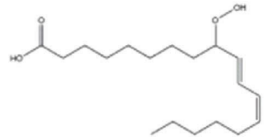
33	(±)9-HODE	22.128	$C_{18}H_{32}O_3$	295.227 87	295.226 77	0.230	295.227 87; 277.217 44; 209.154 94	Neg	Organic acids	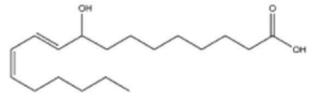
34	(±)13-HODE	23.024	$C_{18}H_{32}O_3$	295.227 91	295.226 77	0.230	295.227 91; 277.217 29; 195.139 01; 171.102 66	Neg	Organic acids	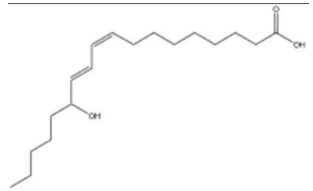
35	(*R*)-3-Hydroxy myristic acid	23.308	$C_{14}H_{28}O_3$	243.197 68	243.195 47	−0.270	243.197 68; 181.160 22; 59.013 87	Neg	Organic acids	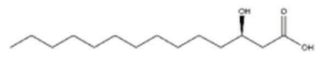
36	6-Methyl [1,2,4] triazolo[4,3-b] pyridazin-8-ol	26.991	$C_6H_6N_4O$	149.046 78	149.045 79	−0.370	149.046 78; 122.035 80; 109.040 91; 106.041 03; 81.045 82	Neg	N-containing organic compounds	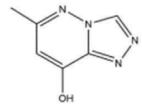

Table 1: Continued.

No.	Compound	t_R(min)	Formula	Measured value (*m/z*)	Theoretical value (*m/z*)	Error (ppm)	Fragment ions (*m/z*)	Mode	Compound type	Structure
37	16-Hydroxyhexadecanoic acid	27.970	$C_{16}H_{32}O_3$	271.228 24	271.226 77	0.810	271.228 24; 253.217 24; 225.222 69; 223.206 92; 71.024 16	Neg	Organic acids	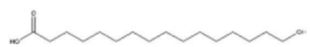
38	*α*-Linolenic acid	28.025	$C_{18}H_{30}O_2$	277.217 35	277.216 21	0.150	277.217 35; 259.205 96	Neg	Organic acids	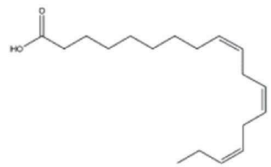
39	2,2′-Methylenebis(4-methyl-6-tert-butylphenol)	29.496	$C_{23}H_{32}O_2$	339.233 22	339.231 86	0.140	339.233 22; 163.11284	Neg	Phenols	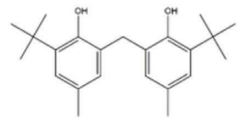
40	9(*Z*),11(*E*)-Conjugated linoleic acid	29.805	$C_{18}H_{32}O_2$	279.233 12	279.231 86	0.390	279.233 12; 261.222 87; 96.969 45	Neg	Organic acids	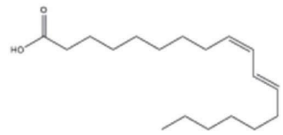
41	Terephthalic acid	30.151	$C_8H_6O_4$	165.019 29	165.018 24	−0.180	165.019 29; 121.029 51; 96.969 59; 77.039 73	Neg	Organic acids	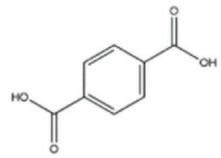
42	Monomethyl phthalate	31.300	$C_9H_8O_4$	179.035 25	179.033 89	−0.220	179.035 25; 135.045 09; 121.029 71; 107.050 29	Neg	Organic acids	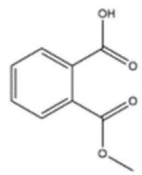
43*	Palmitic acid	31.420	$C_{16}H_{32}O_2$	255.233 17	255.231 86	0.840	255.233 17	Neg	Organic acids	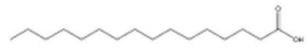
44	Oleic acid	31.830	$C_{18}H_{34}O_2$	281.248 78	281.247 51	0.840	281.148 78; 96.969 64	Neg	Organic acids	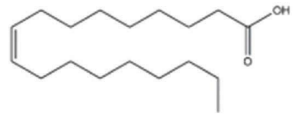
45	Arjungenin	32.333	$C_{30}H_{48}O_6$	503.338 41	503.336 72	1.180	503.338 41; 485.325 44; 471.311 55; 193.050 60; 175.040 02	Neg	Triterpenoid	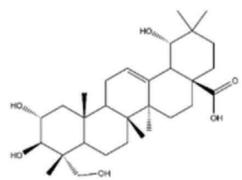

Table 1: Continued.

No.	Compound	t_R(min)	Formula	Measured value (*m/z*)	Theoretical value (*m/z*)	Error (ppm)	Fragment ions (*m/z*)	Mode	Compound type	Structure
46	Choline	0.654	$C_5H_{13}NO$	104.107 31	104.106 99	−0.006	60.081 54; 58.065 89	Pos	N-containing organic compounds	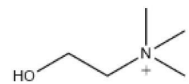
47	Adenosine	0.839	$C_{10}H_{13}N_5O_4$	268.103 88	268.104 03	−0.002	137.045 90; 136.061 83; 119.035 43; 109.051 18	Pos	N-containing organic compounds	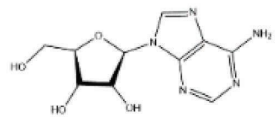
48	*L*-(+)-Leucine	0.871	$C_6H_{13}NO_2$	131.977 40	132.101 91	0.036	86.096 99	Pos	Amino acids	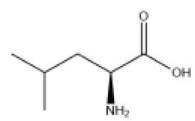
49	*L*-Pyroglutamic acid	0.877	$C_5H_7NO_3$	130.158 97	130.049 87	0.003	113.963 91; 102.956 42	Pos	Amino acids	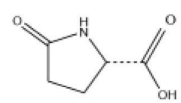
50	*L*-phenylalanine	0.987	$C_9H_{11}NO_2$	166.086 03	166.086 26	0.029	131.049 27; 120.080 99; 103.054 60; 93.070 36	Pos	Amino acids	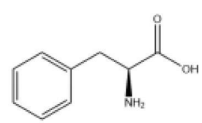
51	*DL*-Tryptophan	1.14	$C_{11}H_{12}N_2O_2$	205.004 32	205.097 15	−0.020	188.070 60; 170.060 07; 159.091 72; 146.070 07; 144.080 87; 143.072 98; 142.065 37; 132.080 87; 130.065 26; 118.065 36; 117.070 07; 115.054 50	Pos	Amino acids	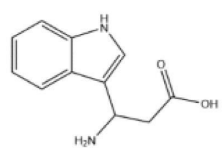
52	Coumarin	4.733	$C_9H_6O_2$	147.044 10	147.044 06	0.027	147.044 10; 119.049 35; 102.989 64; 92.057 93; 91.054 71; 64.927 98	Pos	Coumarin	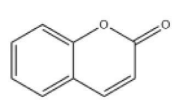
53	4-Phenyl-3-buten-2-one	6.52	$C_{10}H_{10}O$	147.080 57	147.080 44	0.873	147.080 00; 129.070 00; 103.040 00; 91.050 00	Pos	Others	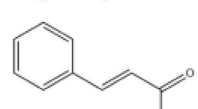
54	Phthalic anhydride	33.88	$C_8H_4O_3$	149.023 33	149.023 32	0.063	149.020 00; 121.030 00; 108.080 00; 98.040 00; 93.060 00	Pos	Others	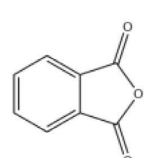

Note: "*" indicates components compared with references.

134.024 52 [M-H-CO_2-CH_3·]$^{-·}$ was obtained. Compared with the reference, peak 20 was identified as ferulic acid.

Peak 11, t_R 1.595, $C_6H_6O_2$, produced ion *m/z* 109.029 49 [M-H]$^-$ in negative mode. Further cleavage produced the secondary fragment ion *m/z* 91.018 82 [M-H-H_2O]$^-$, 81.034 61 [M-H-CO]$^-$, 65.014 47 [M-H-CO_2]$^-$. Combined with the standards online database and the information in the MassBank database and literature, peak 11 was identified as catechol.

Peak 13, t_R 2.007, and peak 14, t_R 2.167, $C_4H_6O_5$, were easily deprotonated in the negative ion mode to produce ion *m/z* 133.014 22 [M-H]$^-$. The main fragment ion peaks in the secondary mass spectrometry were *m/z* 115.003 65 [M-H-H_2O]$^-$, 89.024 48 [M-H-CO_2]$^-$, 87.008 74, 72.993 16, and 71.013 90 [M-H-H_2O-CO_2]$^-$. Combining the information with the standards online database, the MassBank database, and the literature, peaks 13 and 14 were identified as malic acid (i.e., they are enantiomers).

Peak 3, t_R 0.951, showed ion at [M-H]$^-$*m/z* 191.056 12 in negative ion mode. Further cleavage produced the secondary fragment ion *m/z* 173.045 41 [M-H-H_2O]$^-$, 127.039 98 [M-H-H_2O-CH_2O_2]$^-$, 111.008 74 [M-H-2H_2O-CO_2]$^-$, 87.008 74, and 85.029 48 [M-H-2H_2O-CO_2-C_2H_2]$^-$. Combining the retention time, fragment information, and characteristic with reference, peak 3 was identified as D- (-) -quinic acid. The secondary mass spectral profile of peak 3 is shown in Figure 3.

Peak 5 was found at 1.000 min, possessing the quasi-molecular ion [M-H]$^-$ at *m/z* 191.019 74. Further cleavage produced the secondary fragment ion *m/z* 173.046 17 [M-H-H_2O]$^-$, 146.938 60 [M-H-CO_2]$^-$, 129.019 18 [M-H-H_2O-CO_2]$^-$, 111.008 75 [M-H-2H_2O-CO_2]$^-$, 102.948 79, 87.008 76, and 85.029 50 [M-H-H_2O-2CO_2]$^-$. Combining the retention time, fragment information, and characteristics with reference, peak 5 was identified as citric acid. The secondary mass spectral profile of peak 5 is shown in Figure 4.

Peak 7 was found at 1.126 min and yielded parent ion [M-H]$^-$*m/z* 117.019 33 in negative ion mode. Further lysis of secondary fragment ion *m/z* 99.008 74 [M-H-H_2O]$^-$, 73.029 46 [M-H-CO_2]$^-$, compared with the standard database, information from MassBank database and references [35], peak 10 was identified as succinic acid. The secondary mass spectrogram of peak 7 is shown in Figure 5.

Peak 8, t_R 1.191, had the deprotonated ions at *m/z* 169.014 14 [M-H]$^-$ in negative ion mode. The daughter ion at *m/z* 125.024 35 is attributed to the loss of CO_2. Combined with the standard database, the MassBank database, and literature information [36], peak 8 was identified as gallic acid. The secondary mass spectral profile of peak 8 is shown in Figure 6.

Peak 15 was found at 2.228 min and yielded parent ion [M-H]$^-$ at *m/z* 153.019 32. Further cleavage generated the daughter ion *m/z* 123.045 17, 109.029 45 [M-H-CO_2]$^-$, and 108.021 45 [M-H-CO_2-H·]$^{-·}$. Combined with the standard database and the information in the MassBank database and literature [37], peak 15 was identified as a gentisic acid. The secondary mass spectral profile of peak 15 is shown in Figure 7.

Peak 18 (t_R 2.859) gave [M-H]$^-$ at *m/z* 179.034 96 in negative ion mode. The daughter ion at *m/z* 135.045 18[M-H-CO_2]$^-$ was attributed to the loss of CO_2. In addition, compared with the information with reference, peak 18 was identified as caffeic acid. The secondary mass spectral map of peak 18 is shown in Figure 8.

3.3.2. Amino Acids. Seven amino acids were identified in the samples. Amino acids often contain -NH_2 and -COOH functional groups. Generally, amino acids lose H_2O or -COOH, and some amino acids lose NH_3. Peaks 4 and 50 are used as examples to explain the lysis rules.

Peak 4 was found at 0.978 min and yielded the parent ion [M-H]$^-$ at *m/z* 131.045 94. Further cleavage produced the daughter ion *m/z* 114.019 65 [M-H-NH_2]$^-$, 113.035 70 [M-H-H_2O]$^-$, 111.020 13, 87.056 59[M-H-CO_2]$^-$, 72.009 07, and 70.029 80 [M-H-CO_2-NH_3]$^-$. Retention time, fragmentation information, and feature peaks matched the information in a local database (mzVault) and the HMDB database. Thus, peak 4 was identified as asparagine. The secondary mass spectral profile of peak 4 is shown in Figure 9.

Peak 50 (t_R 0.987) was found in positive ion mode, generating [M + H]$^+$ at *m/z* 166.086 03. Further lysis produced *m/z* 131.049 27, 120.080 99, 103.054 60, 93.070 36. Combined with the reference and MassBank database, peak 50 was identified as L-phenylalanine. The secondary mass spectral profile of peak 50 is shown in Figure 10.

3.3.3. Fatty Acids. Two fatty acids were identified (palmitic and oleic acid). Palmitic acid was identified by combining with reference and database and was found at 31.420 min in negative ion mode, yielding parent ion [M-H]$^-$ at *m/z* 255.233 17. Further lysis produced secondary fragment *m/z* 236.902 79 [M-H-H_2O]$^-$. Peak 43 had the corresponding character when compared with references and databases. Therefore, peak 43 was identified as palmitic acid. Its secondary mass spectrometry is shown in Figure 11. Oleic acid was identified by combining the standard database, MassBank database, and related literature [38]. Peak 44 was found at 31.830 min, produced [M-H]$^-$ peak at *m/z* 281.248 75, and matched the database and literature information. Thus, peak 44 was identified as oleic acid.

3.4. Method Validation for Quantitation of Three Compounds. Regression equations were obtained by plotting corresponding peak areas versus different concentrations. All the regression equations exhibited excellent linearity, the values of linear ranges (r^2) from analytical curves were >0.999 and linearity equations were listed in Table 2. RSDs of the precision test ranged from 0.9% to 1.7%. In addition, the accuracy of the proposed method was assessed. The results indicated that the UHPLC Q-Exactive Orbitrap method possessed good accuracy with recoveries ranging from 103.0% to 104.8%, while all RSDs were less than 3%. The optimized and validated UHPLC Q-Exactive-Orbitrap method was used for quantitative analysis. The contents of the three compounds are listed in Table 2.

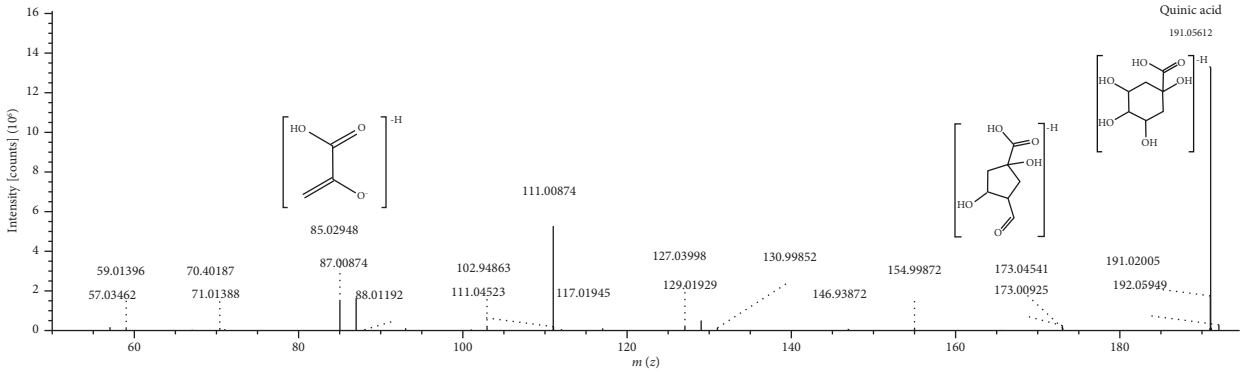

Figure 3: The MS^2 mass spectrum of peak 3 in the negative ion mode.

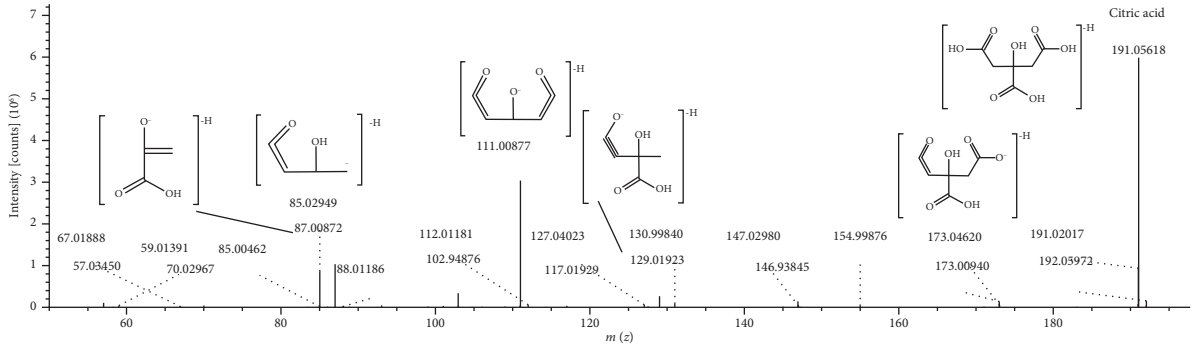

Figure 4: The MS^2 mass spectrum of peak 5 in the negative ion mode.

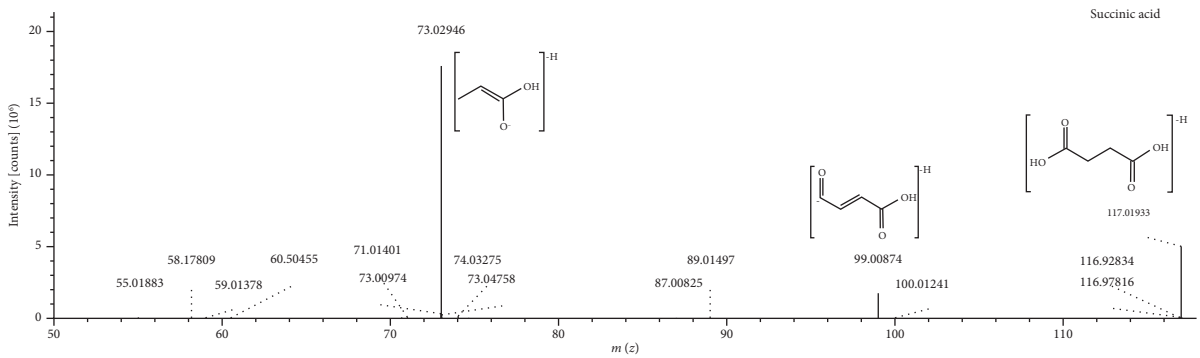

Figure 5: The MS^2 mass spectrum of peak 7 in the negative ion mode.

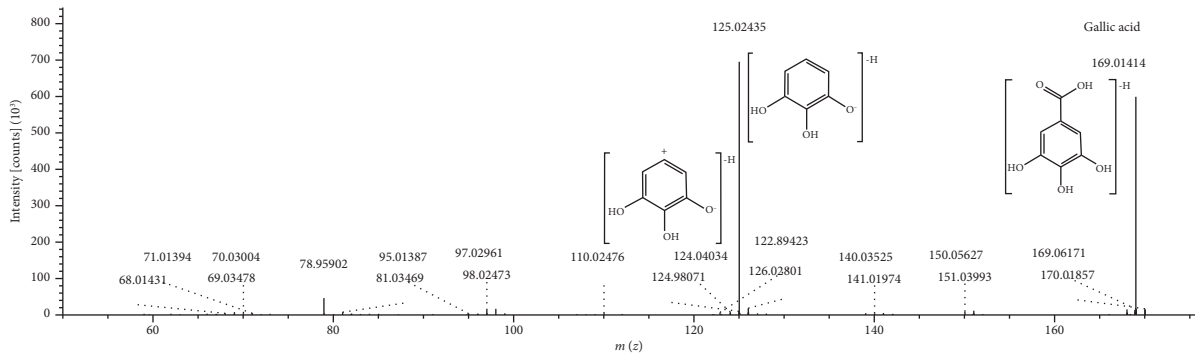

Figure 6: The MS^2 mass spectrum of peak 8 in the negative ion mode.

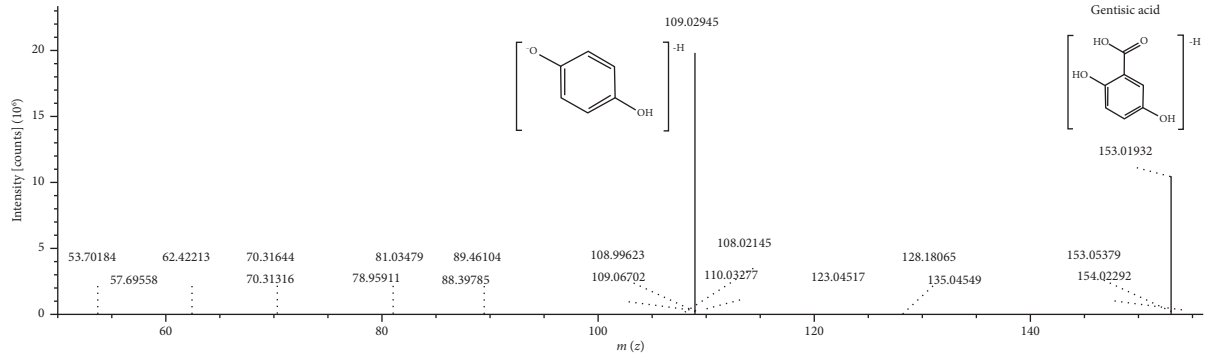

Figure 7: The MS^2 mass spectrum of peak 15 in the negative ion mode.

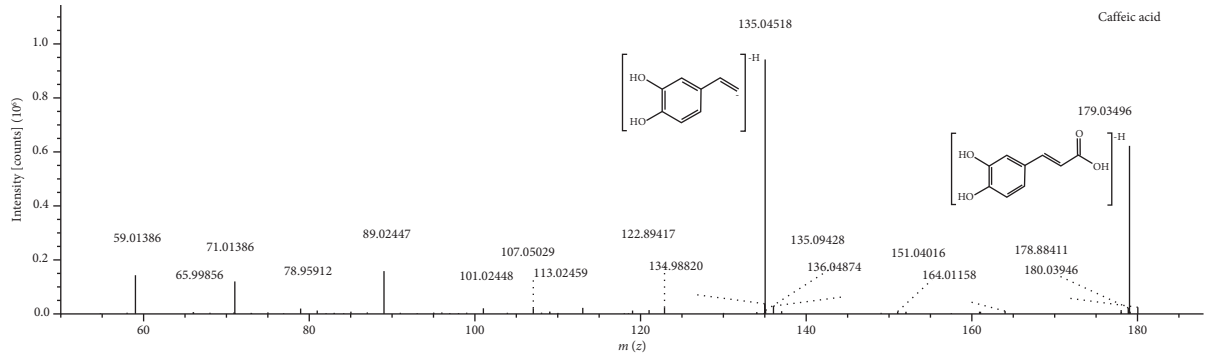

Figure 8: The MS^2 mass spectrum of peak 18 in the negative ion mode.

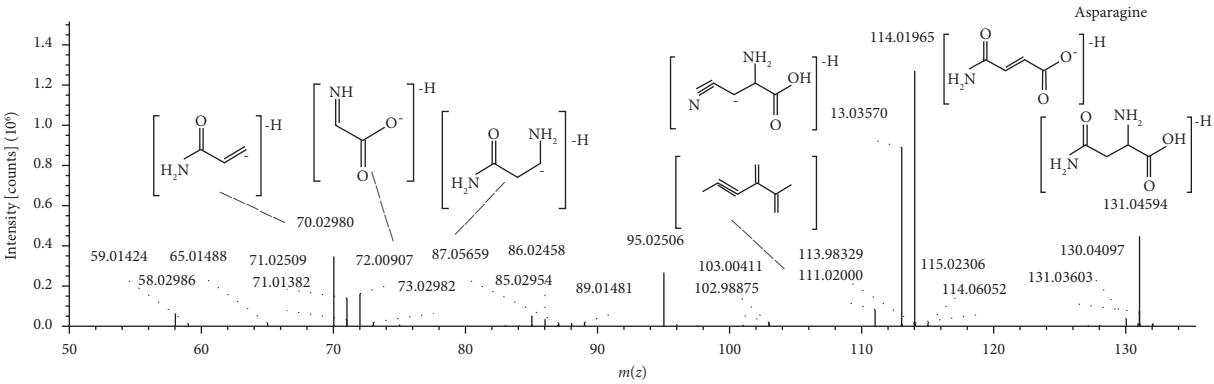

Figure 9: The MS^2 mass spectrum of peak 4 in the negative ion mode.

4. Discussion

UHPLC Q-Exactive Orbitrap MS technology is characterized by high resolution, fast analysis speed, and good sensitivity. It is a necessary means to analyze small molecule compounds. Using UHPLC Q-Exactive Orbitrap MS technology for the first time, this study systematically characterized the chemical profile of *Canna edulis* Ker-Gawl. After optimizing the method, we selected pure methanol as the extraction solvent and acetonitrile 0.1% formic acid water as the mobile phase. In this study, we identified 54 compounds from methanol extracts and carried out

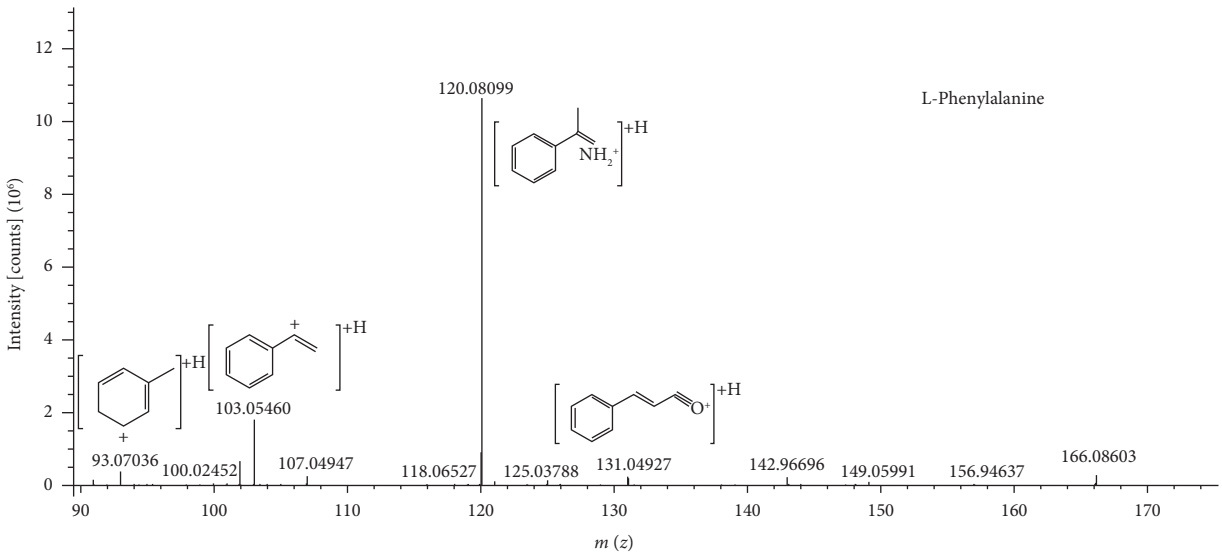

Figure 10: The MS^2 mass spectrum of peak 50 in the positive ion mode.

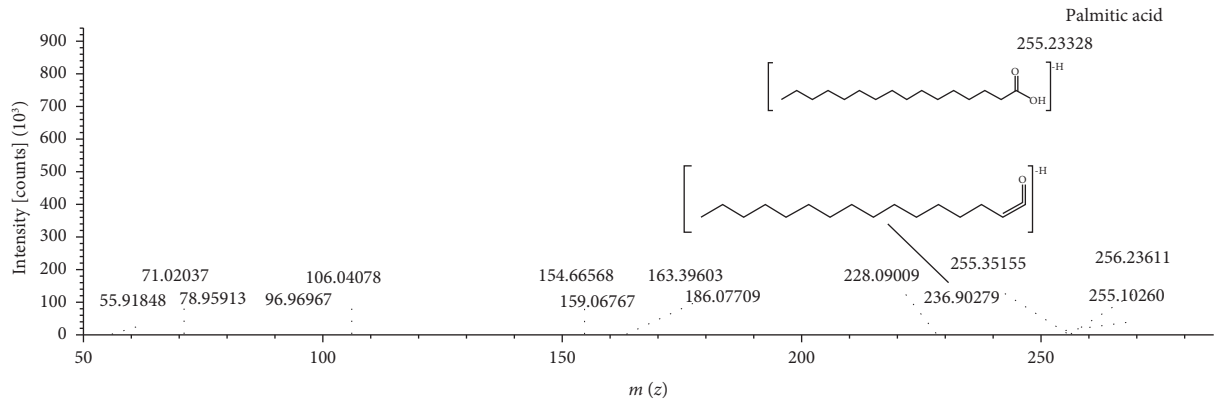

Figure 11: The MS^2 mass spectrum of peak 43 in the negative ion mode.

quantitative analysis and methodological validation on three of them. This study identified more peaks and compounds in negative ion mode. Forty-five chemical components (mainly organic acid components) were identified in negative ion mode, and nine chemical components (mainly amino acid components) were identified in positive ion mode. Most of the identified compounds have good biological activity, such as, caffeic acid, gallic acid, gentisic acid, ferulic acid, and other phenolic compounds. Moderate intake of these compounds can present promising effects in the prevention of diseases [17, 39–41] such as diabetes, obesity, Parkinson's, cardiovascular disease, and others. In view of antioxidant activity, these compounds can be developed as natural food additives [31, 42, 43].

Plants of the homologous family contain parent nuclei of similar compositions. According to the literature, *Canna edulis* Ker is a cultivarietas of *Canna indica* L. Studies have found that *Canna indica* Linn. (Cannaceae) contains flavonoids, polyphenols, essential oils, and anthocyanins [44–49]. These chemical components were not identified in this study. The possible reasons are changes in chemical composition due to processing, low content, and difficulty

Table 2: Method validation.

Compounds	Regression equations	Linearity (r^2)	Linear range (μM)	LODs (ng/mL)	LOQs (ng/mL)	Precision (RSD, %, $n = 6$)	Accuracy (RSD, %, $n = 9$)	Recovery rate (%)	Content (mg/g)
D-(-)-quinic acid	$y = 13397835^{*}x + 10108567$	0.9998	0.781-50.000	0.015	0.050	1.2	0.7	104.8	0.076
Caffeic acid	$y = 14778853^{*}x + 114694406$	0.9991	7.813–500.000	0.703	2.350	1.7	0.8	103.0	0.110
Ferulic acid	$y = 984823^{*}x + 1353717$	0.9995	0.260-16.667	0.038	0.126	0.9	2.4	103.3	0.003

ionizing in this ion mode. To characterize the components of *Canna edulis* Ker-Gawl, molecular networks with the GNPS database and other technical methods can be used.

5. Conclusion

In this study, the UHPLC Q-Exactive Orbitrap MS method was used for the first time to accurately, quickly, and systematically characterize the compounds of the rhizome of *Canna edulis* Ker-Gawl. 54 chemical constituents were identified from the methanol extract of the rhizome, including 36 organic acids (with six phenolic acids), three phenols, one sugar (and its derivatives), one coumarin, one triterpenoid, ten N-containing organic compounds (including seven amino acids), and two other compounds. Moreover, three compounds were quantitatively analyzed and a methodological study was carried out. The established method provided satisfactory precision and accuracy, acceptable recovery, a good linearity and a reasonable detection limit. We preliminarily revealed the pharmacodynamic substance basis of this rhizome and provided a basis for quality control, in-depth research, and development.

Data Availability

The data used to support the findings of this study are included within the article.

Conflicts of Interest

The authors declare that there are no conflicts of interest regarding this study.

Acknowledgments

This study was funded by the Special Investigation of Science and Technology Basic Resources (Grant no. 2018FY100704) and Science and Technology Program Project of Guizhou Province (Grant no. [2020]4Y074).

References

[1] H. Tang, F. Peng, and T. Zhnag, "Cultivation and demonstration of canna taro varities in southwest of Guizhou," *Tillage and Cultivation*, vol. 40, no. 4, pp. 63-64, 2020.

[2] J. Zhao, X. Gu, and J. Su, "Determination of the amount of K, Na, Ca and Zn in canna edulis ker," *Guangzhou Chemical Industry*, vol. 43, no. 20, pp. 144–146+66, 2015.

[3] W. E. Zhang, F. Wang, and X. Pan, "Accumulation and translocation properties of dry matter and mineral elements in edible canna(Canna edulis Ker)," *Journal of Plant Nutrition and Fertilizer*, vol. 19, no. 3, pp. 670–676, 2013.

[4] W. E. Zhang and X. Pan, "Absorption accumulation and transport of trace elements of Canna edulis Ker at different growth stages," *Jiangsu Agricultural Sciences*, vol. 44, no. 7, pp. 262–265, 2016.

[5] J. Zhang, F. Chen, F. Liu, and Z. W. Wang, "Study on structural changes of microwave heat-moisture treated resistant Canna edulis Ker starch during digestion in vitro," *Food Hydrocolloids*, vol. 24, no. 1, pp. 27–34, 2010.

[6] J. Zhang and Z.-W. Wang, "Optimization of reaction conditions for resistant Canna edulis Ker starch phosphorylation and its structural characterization," *Industrial Crops and Products*, vol. 30, no. 1, pp. 105–113, 2009.

[7] P. V. Hung and N. Morita, "Physicochemical properties and enzymatic digestibility of starch from edible canna (Canna edulis) grown in Vietnam," *Carbohydrate Polymers*, vol. 61, no. 3, pp. 314–321, 2005.

[8] E. Perez and M. Lares, "Chemical composition, mineral profile, and functional properties of Canna (Canna edulis) and Arrowroot (Maranta spp.) starches," *Plant Foods for Human Nutrition*, vol. 60, no. 3, pp. 113–116, 2005.

[9] J. R B Witono, H. Santoso, Y. I. P. Arry Miryanti, and D. Tan, "Integration of physical and chemical treatment on the extraction of starch from Canna edulis Ker. rhizome," *Agricultural Sciences*, vol. 4, no. 9, pp. 51–55, 2013.

[10] S. Handajani and L. T. Pangesthi, "Optimization of ganyong starch (canna edulis) on making of dry and instant noodles," *IOP Conference Series: Earth and Environmental Science*, vol. 347, no. 1, Article ID 012082, 2019.

[11] J. Zhang and Z. W. Wang, "Soluble dietary fiber from Canna edulis Ker by-product and its physicochemical properties," *Carbohydrate Polymers*, vol. 92, no. 1, pp. 289–296, 2013.

[12] R. Kartika, I. P. Sukanadi, and A. S. Prasetya, "Utilization tofu dregs as a source of nitrogen in fermentation of tuber ganyong (Canna edulis kerr.) by saccharomyces cerevisiae," *International Journal of Scientific and Technology Research*, vol. 8, no. 8, pp. 1054–1057, 2019.

[13] W. E. Zhang, X. Pan, and B. Guo, "Analysis on the main components of the rhizome of the main Canna edulis lines in Xingyi City," *Tillage and Cultivation*, vol. 5, pp. 14–32, 2008.

[14] Y. Huang, Y. Jin, Y. Fang, Y. Li, and H. Zhao, "Simultaneous utilization of non-starch polysaccharides and starch and viscosity reduction for bioethanol fermentation from fresh Canna edulis Ker. tubers," *Bioresource Technology*, vol. 128, no. 2013, pp. 560–564, 2013.

[15] R. Najini, M. S. Bachri, and S. Yuliani, "The gastroprotective effects of Canna edulis ker. tuber starch on peptic ulcer and the histopathological profile of rat stomach," *Pharmacia*, vol. 8, no. 1, p. 43, 2018.

[16] M. Burhannudin, N. Mahmudah, S. Widyarini, and D. Purnomosari, "Chemopreventive effects of edible canna (canna edulis kerr.) against colorectal carcinogenesis: effects on expression of adenomatous polyposis coli and inducible nitric oxide synthase in rat inflammatory model," *Asian Pacific Journal of Cancer Prevention*, vol. 19, no. 3, pp. 839–844, 2018.

[17] T. M. H. Nguyen, H. L. Le, T. T. Ha et al., "Inhibitory effect on human platelet aggregation and coagulation and antioxidant activity of *C. edulis* Ker Gawl rhizome and its secondary metabolites," *Journal of Ethnopharmacology*, vol. 263, no. 2020, pp. 113136–113145, 2020.

[18] T. M. H. Nguyen, H. L. Le, Q. H. Tran et al., "Data on antiplatelet aggregation, anticoagulation and antioxidant activities of Canna edulis Ker rhizome and its secondary metabolites," *Data in Brief*, vol. 32, no. 2020, pp. 106115–106132, 2020.

[19] J. Zhang and Z.-W. Wang, "Soluble dietary fiber from canna edulis ker by-product and its enzymatic and antioxidant activities," *Food Biotechnology*, vol. 25, no. 4, pp. 336–350, 2011.

[20] J. Zhang, Z.-W. Wang, and Q. Mi, "Polyphenol oxidase inhibitory and antioxidant activity of extract of Canna edulis ker

stem," *Journal of Food Biochemistry*, vol. 35, no. 4, pp. 1342–1360, 2011.

[21] M. Qiu, X. Jin, and C. Zhang, "Effect of canna edulis type 3 resistant starch in reducing body weight, serum lipid and acute toxicity," *Chinese Journal of Experimental Traditional Medical Formulae*, vol. 25, no. 1, pp. 149–156, 2019.

[22] J. Wu, M. Qiu, C. Zhang et al., "Type 3 resistant starch from Canna edulis modulates obesity and obesity-related low-grade systemic inflammation in mice by regulating gut microbiota composition and metabolism," *Food and Function*, vol. 12, no. 23, pp. 12098–12114, 2021.

[23] C. Zhang, S. Ma, J. Wu et al., "A specific gut microbiota and metabolomic profiles shifts related to antidiabetic action: the similar and complementary antidiabetic properties of type 3 resistant starch from Canna edulis and metformin," *Pharmacological Research*, vol. 159, Article ID 104985, 2020.

[24] C. Zhang, M. Qiu, T. Wang et al., "Preparation, structure characterization, and specific gut microbiota properties related to anti-hyperlipidemic action of type 3 resistant starch from Canna edulis," *Food Chemistry*, vol. 351, no. 2021, Article ID 129340, 2021.

[25] C. Zhang, L. Dong, J. Wu et al., "Intervention of resistant starch 3 on type 2 diabetes mellitus and its mechanism based on urine metabonomics by liquid chromatography-tandem mass spectrometry," *Biomedicine & Pharmacotherapy*, vol. 128, Article ID 110350, 2020.

[26] C. Luo, F. Liu, and L. Yang, "Description and data collection in main traits of canna delis germplasm resource," *Journal of Anhui Agri*, vol. 45, no. 10, pp. 16–18, 2017.

[27] G. Ou, L. Yang, and C. Luo, "Ecological production technology of canna edulis ker in Guizhou," *Agricultural Technology Service*, vol. 36, no. 1, pp. 22–25, 2019.

[28] W. Wei, "Application of canna edulis resistant starch in hypoglycemic noodles," *Modern Food*, vol. 18, pp. 65–70, 2019.

[29] J. D. Guzman-Vasquez and L. E. Cuca-Suarez, "Estudio químico de algunos metabolitos secundarios aislados de la parte aérea de Canna edulis Ker Gawl," *Actualidades Biológicas*, vol. 27, no. 1, pp. 91–94, 2018.

[30] Y. Sook Yun, M. Satake, S. Katsuki, and A. Kunugi, "Phenylpropanoid derivatives from edible canna, Canna edulis," *Phytochemistry*, vol. 65, no. 14, pp. 2167–2171, 2004.

[31] J. Zhang, Z.-W. Wang, and Q. Mi, "Phenolic compounds from Canna edulis Ker residue and their antioxidant activity," *LWT-Food Science and Technology*, vol. 44, no. 10, pp. 2091–2096, 2011.

[32] J. Zhang, P. D. Paré, and A. J. Sandford, "Recent advances in asthma genetics," *Respiratory Research*, vol. 9, no. 1, p. 4, 2008.

[33] Y. Wang and F. Ye, "Thermo scientific Q exactive," *China Food*, vol. 22, pp. 64-65, 2011.

[34] B. Zeng, H. Liu, and X. Liu, "Application of UPLC-Q-exactive Orbitrap MS technology in the analysis of traditional Chinese medicine," *Journal of Chinese Medicinal Materials*, vol. 9, pp. 2313–2319, 2020.

[35] J. Shi, S. Zhang, and Z. Chai, "Analysis of chemical constituents in qizhi jiangtang capsules based on UPLC-QE-orbitrap-MS," *Chinese Journal of Experimental Traditional Medical Formulae*, vol. 27, no. 16, pp. 116–123, 2021.

[36] L. Chen, Y. Wang, and F. Feng, "Analysis on chemical components of yangyinqingfei oral liquid by UPLC-Q-exactiveorbitrap-MS," *Guangzhou Chemical Industry*, vol. 47, no. 9, pp. 118–123, 2019.

[37] X. Wang, J. Hu, and H. Ren, "Chemical constituents in porana racemosa roxb. By UPLC-Q-exactive focus-MS/MS," *Central South Pharmacy*, vol. 20, no. 1, pp. 52–59, 2022.

[38] M. Abe, Y. Ito, A. Suzuki, S. Onoue, H. Noguchi, and S. Yamada, "Isolation and pharmacological characterization of fatty acids from saw palmetto extract," *Analytical Sciences*, vol. 25, no. 4, pp. 553–557, 2009.

[39] O. M. Agunloye, G. Oboh, A. O. Ademiluyi et al., "Cardio-protective and antioxidant properties of caffeic acid and chlorogenic acid: mechanistic role of angiotensin converting enzyme, cholinesterase and arginase activities in cyclosporine induced hypertensive rats," *Biomedicine & Pharmacotherapy*, vol. 109, pp. 450–458, 2019.

[40] M. B. Sanchez, E. Miranda-Perez, J. C. G. Verjan, M. de los Angeles Fortis Barrera, J. Perez-Ramos, and F. J. Alarcon-Aguilar, "Potential of the chlorogenic acid as multitarget agent: insulin-secretagogue and PPAR α/γ dual agonist," *Biomedicine & Pharmacotherapy*, vol. 94, pp. 169–175, 2017.

[41] V. Dayu Putri and F. Dyna, "Standarisasi ganyong (canna edulis ker) sebagai pangan alternatif pasien diabetes mellitus," *Jurnal Katalisator*, vol. 4, no. 2, p. 111, 2019.

[42] H. Minantyo, K. Audrey, and V. Yuwono, "Komposisi dodol ganyong (canna edulis ker), tape ketan hitam, sari kedelai ditinjau Dari uji organoleptik," *TEKNOBUGA: Jurnal Teknologi Busana dan Boga*, vol. 9, no. 1, pp. 47–53, 2021.

[43] T. Mishra, A. Das, and A. Sen, "Phytochemical screening and ln-vitro antioxidant profiling of solvent fractions of canna edulis ker gawler," *Free Radicals and Antioxidants*, vol. 2, no. 1, pp. 13–20, 2012.

[44] X. Tang, J. Liu, and Z. Zhang, "Studies on the chemical constituents of Canna," *Chinese Traditional and Herbal Drugs*, vol. 26, no. 2, p. 107, 1995.

[45] P. S. Vankar and J. Srivastava, "Comparative study of total phenol, flavonoid contents and antioxidant activity in canna indica and Hibiscus rosa sinensis: prospective natural food dyes," *International Journal of Food Engineering*, vol. 4, no. 3, 2008.

[46] J. Purintrapiban, M. Suttajit, and N. E. Forsberg, "Differential activation of glucose transport in cultured muscle cells by polyphenolic compounds from canna indica L. Root," *Biological and Pharmaceutical Bulletin*, vol. 29, no. 10, pp. 1995–1998, 2006.

[47] J. Srivastava and P. S. Vankar, "Methylated anthocyanidin glycosides from flowers of Canna indica," *Carbohydrate Research*, vol. 345, no. 14, pp. 2023–2029, 2010.

[48] S. T. Kumbhar, S. P. Patil, and H. D. Une, "Phytochemical analysis of Canna indica L. roots and rhizomes extract," *Biochemistry and biophysics reports*, vol. 16, pp. 50–55, 2018.

[49] D. Kong, Y. Li, and C. Fan, "GC-MS analysis of Canna indica L. leaf volatile oil," *Modern Chinese Medicine*, vol. 15, no. 6, pp. 445–447, 2013.